

Article

Not peer-reviewed version

---

# Application of Laser Particle Size Analyzer to Evaluation of Batch Consistency and Stability of Aluminum Adjuvant Adsorbed Vaccine

---

[Li Xinwei](#) , Fang Wei , Wang Enna , Zeng Haiyuan , [Song Jie](#) , [Wu Fan](#) , [Su Wen](#) \*

Posted Date: 6 May 2026

doi: 10.20944/preprints202605.0365.v1

Keywords: laser diffraction particle size analyzer; aluminum adjuvant; adsorbed vaccine; EV71 vaccine; DTaP vaccine; particle size; storage stability



Preprints.org is a free multidisciplinary platform providing preprint service that is dedicated to making early versions of research outputs permanently available and citable. Preprints posted at Preprints.org appear in Web of Science, Crossref, Google Scholar, Scilit, Europe PMC, OpenAlex.

Copyright: This open access article is published under a [Creative Commons CC BY 4.0 license](#), which permit the free download, distribution, and reuse, provided that the author and preprint are cited in any reuse.

Disclaimer/Publisher's Note: The statements, opinions, and data contained in all publications are solely those of the individual author(s) and contributor(s) and not of MDPI and/or the editor(s). MDPI and/or the editor(s) disclaim responsibility for any injury to people or property resulting from any ideas, methods, instructions, or products referred to in the content.

Article

# Application of Laser Particle Size Analyzer to Evaluation of Batch Consistency and Stability of Aluminum Adjuvant Adsorbed Vaccine

Li Xinwei <sup>1</sup>, Fang Wei <sup>1</sup>, Wang Enna <sup>1</sup>, Zeng Haiyuan <sup>1</sup>, Song Jie <sup>2</sup>, Wu Fan <sup>1</sup> and Su Wen <sup>1,\*</sup>

<sup>1</sup> Yunnan Institute for Food and Drug Control, Ministry of Industry and Information Technology Industrial Technology Basic Public Service Platform, Kunming, China

<sup>2</sup> China Institute of Medical Biology, Chinese Academy of Medical Sciences, Kunming, China

\* Correspondence: llfj-007@163.com; Tel.: +86-1388852061,650000

## Abstract

**Background/Objectives:** Aluminum-adsorbed vaccines are widely used in pediatric immunization, yet particle size and distribution are critical but under-standardized quality attributes. **Methods:** This study aimed to establish and validate a laser diffraction particle size analysis for evaluating particle size consistency and stability of inactivated enterovirus 71 (EV71) vaccine and adsorbed acellular diphtheria–tetanus–pertussis (DTaP) vaccine. **Results:** EV71 vaccine stock solution (40–350 nm) and aluminum adjuvant (75–600 nm) exhibited distinct distributions, with the final product showing bimodal distribution (50–14,000 nm): main peak at 0.1–0.2  $\mu\text{m}$  (~65%) and secondary peak at 0.3–3  $\mu\text{m}$  (~14%). DTaP final product (2000–20,000 nm) showed significant aggregation with 79.6% at 3–8  $\mu\text{m}$  and 15.7% at >8  $\mu\text{m}$ . Four EV71 batches (A1–A4) showed uneven inter-batch consistency (D50: 100, 132, 103, 103 nm; CV 13.8%), while intra-batch CVs were acceptable (3.9% for EV71, 8.0% for DTaP). Long-term stability at 4 °C revealed gradual aggregation: EV71 D50 increased from 100 nm to 134 nm over 60 days, with >0.2  $\mu\text{m}$  aggregates increasing from 0.03% to 1.50%; DTaP showed severe tailing at day 60 (>50  $\mu\text{m}$  particles: 2.8%). Accelerated studies showed 37 °C caused slight enlargement, whereas –20 °C induced marked aggregation (EV71 D50: ~37  $\mu\text{m}$ , CV 16.1%; DTaP D50: ~45  $\mu\text{m}$ , CV 13.8%). **Conclusions:** Laser particle size analysis is a robust, reliable tool for assessing particle size consistency and stability of aluminum-adsorbed vaccines. It supports process control, batch release, and stability monitoring to improve vaccine quality and safety.

**Keywords:** laser diffraction particle size analyzer; aluminum adjuvant; adsorbed vaccine; EV71 vaccine; DTaP vaccine; particle size; storage stability

## 1. Introduction

The inactivated Enterovirus 71 (EV71) vaccine is a vaccine adsorbed with EV71 inactivated virus by aluminium adjuvant, which is used to prevent hand-foot-mouth disease (HFMD) caused by EV71 infection[1–3]. The adsorbed diphtheria, tetanus and pertussis vaccine (DTP) is also a combined vaccine made by adsorbing pertussis vaccine (P), diphtheria toxoid vaccine (D) and tetanus toxoid vaccine (T) with aluminium adjuvant. It is used to prevent diseases caused by *Bordetella pertussis*, *Corynebacterium diphtheriae* and *Clostridium tetani* in infants and young children[4,5]. Among them, pertussis vaccine includes whole cell pertussis vaccine (WPV) and acellular pertussis vaccine (APV), so DTP vaccine is divided into DTaP and DTwP[6,7]. Due to the lower side effects of DTaP compared with DTwP, but higher production cost, DTaP has been fully used to replace DTwP in many countries[8,9].

As a limited means for disease prevention and control, vaccines are mostly administered to specific healthy populations. Therefore, the safety and efficacy of vaccines are of paramount importance[10]. To ensure the safety and efficacy of vaccines throughout their entire life cycle, it is

necessary to study the stability of vaccines[11]. Among them, the size of vaccine particles can serve as an important indicator of production process consistency and product stability, and is also an important attribute for vaccine quality evaluation[12]. Currently, there are multiple methods for detecting the size and distribution of vaccine particles, such as Dynamic Light Scattering (DLS)[13], Laser Diffraction[14], Electron Microscopy (EM)[15], and High Performance Liquid Chromatography (HPLC) combined with Size Exclusion Chromatography (SEC)[16]. However, the Chinese Pharmacopoeia (2025 Edition) [17] has not yet specified the detection methods for the size and distribution of vaccine particles. Only the detection methods for subvisible particles (SVP) are specified as light obscuration (LO)[18] and optical microscopy method[19]. However, both of these methods have limitations such as a narrow detection range and inability to cover the distribution range of vaccine particles[20]. And aluminum adjuvant adsorbed vaccines[21], represented by EV71 and DPT vaccines, are prone to rapid particle sedimentation, which affects the routine detection of vaccine particle size[22]. With the continuous improvement of vaccine quality evaluation standards, there is an urgent need for a new method to evaluate the particle size distribution of vaccines.

Dynamic light scattering can detect particles smaller than 1 nm in size and is suitable for measuring the particle size and distribution of molecules and particles in the submicron range[23]. Dynamic laser scattering method can be used for the characterization of biological macromolecules such as proteins, antibodies, and viruses. Its advantages lie in its speed, non-destructiveness, and the ability to measure extremely small particles. The principle is that when nanoparticles are suspended in a liquid, they undergo Brownian motion (where the particles move randomly and irregularly due to the thermal collisions of solvent molecules). The speed of the particles' Brownian motion is related to their size, the smaller the particle, the faster it moves. The laser particle size analyzer measures the particle size by utilizing the phenomenon of scattering (diffraction) that occurs when a laser beam shines on the particles. The particle size is determined based on the distribution of the scattered (diffracted) light intensity. The particles to be measured are dispersed in the scanning path of the laser. As the laser travels, it encounters the particles and, according to the Mie scattering theory, when the radius of the particle is close to or greater than the wavelength of the incident light, most of the incident light will undergo scattering in the direction of its travel. After scattering, some of the light deviates from the original propagation direction. Based on the scattering law, the smaller the particle size, the greater the deviation. The larger the particle size, the smaller the deviation. The calculation formula is the Stokes-Einstein equation, where  $D$  represents the translational diffusion coefficient,  $k_B$  is the Boltzmann constant,  $T$  is the absolute temperature,  $\eta$  is the solvent viscosity, and  $d_h$  is the hydrodynamic diameter (measured result)[24,25].

$$D = \frac{k_B T}{3\pi\eta d_h}$$

Therefore, in this study, laser diffraction was used to analyze the particle size of EV71 vaccine and DTaP vaccine stock solutions, their adjuvants and the final vaccine products, to study the consistency and stability of vaccine particles, explore the adsorption effect of aluminum adjuvant vaccines on antigen proteins, evaluate the particle consistency between vaccine batches, and the stability of particles during long-term and accelerated storage.

## 2. Materials and Methods

### 2.1. Samples

Samples of final EV71 vaccine products (batch numbers A1-A4) from Factory A, a batch of EV71 vaccine stock solution and aluminum adjuvant, and final DTaP vaccine products (batch number B1) from Factory B, along with the vaccine stock solution of pertussis vaccine, diphtheria toxoid vaccine and tetanus toxoid vaccine, were all provided by the Biological Product Certification Institute of Yunnan Provincial Food and Drug Supervision and Inspection Bureau. All samples were stored at 4 °C.

## 2.2. Main Instruments

The laser particle size measurement system (main unit model: S3500, analysis software: Microtrac Flex) is provided by Microtrac (USA).

The desk scanning electron microscope (main unit model: TM4000ii plus, analysis software: TM4000 Information Collector) is provided by Hitachi High-Technologies Corporation (Japan).

## 2.3. Measurement Method of Laser Particle Size Analyzer

The S3500 laser particle size analyzer is used to measure the particle size and distribution of the sample to be tested. The sample is injected into the sample chamber, and it is ultrasonically dispersed in the liquid (purified water). The pumped circulation passes through the measurement chamber. The laser beam is collimated by a lens and then irradiates the sample chamber (wet method). The refractive indices of the sample and the dispersing medium (water is used as the dispersing medium, and the refractive index is generally taken as 1.33) are input. Microtrac Flex calculates the particle size distribution through an inversion algorithm and outputs parameters such as D10/D50/D90.

## 2.4. Measurement Method of Desktop Scanning Electron Microscope

Use the TM4000ii plus desktop scanning electron microscope to detect the microscopic images of the sample. Attach the dry and conductive sample to the sample stage, push it into the chamber and evacuate the air. Select the target area in the low-magnification navigation window, switch to high-magnification image, adjust the brightness and contrast to the best level, and then save the image.

## 2.5. Methodological Validation of the Instrument

Since there were no corresponding particle size reference materials for the two vaccines, and the particle size range of polystyrene microspheres was similar to that of the test samples, the accuracy and reproducibility of the method were verified using the certified reference material of polystyrene microspheres. Certified reference materials with D50 values of 10  $\mu\text{m}$  and 25  $\mu\text{m}$  (provided by Beijing Haian Honghong Standard Substance Technology Co., Ltd., batch numbers: GBW(E)120024, GBW(E)120027) were selected to represent two regions of the vaccine particle size. The S3500 laser particle size analyzer was used to repeat the measurement 6 times. The relative error (RE) and Relative Standard Deviation (RSD) of D50 for the two reference materials were calculated. Acceptance criteria: The absolute value of RE for accuracy D50 should be  $< 0.05\%$ , and the RSD for reproducibility D50 should be  $< 5\%$ .

The two certified reference materials of D50 were re-determined 6 times each, and the  $|RE|$  values of D50 were all  $< 5.00\%$ , and the RSD values were all  $< 5.00\%$ , all within the acceptable standard range, as shown in Table 1. This indicated that the accuracy and reproducibility of the method were good.

**Table 1.** Verification for accuracy and reproducibility of laser particle size analyzer for determination of D50 of two kinds of standards.

| Certified reference materials | The results of D50 ( $\mu\text{m}$ ) |       |       |       |       |       | Average value | RE(%) | RSD(%) |
|-------------------------------|--------------------------------------|-------|-------|-------|-------|-------|---------------|-------|--------|
|                               | 1                                    | 2     | 3     | 4     | 5     | 6     |               |       |        |
| 10 $\mu\text{m}$              | 10.35                                | 10.35 | 10.35 | 10.36 | 10.35 | 10.34 | 10.35         | 3.50  | 0.06   |
| 25 $\mu\text{m}$              | 23.99                                | 24.07 | 24.07 | 24.02 | 24.00 | 24.05 | 24.03         | 3.87  | 0.15   |

## 2.6. Analysis and Evaluation

### 2.6.1. Analysis of the Adsorption Effect of Aluminum Adjuvant on Antigen Protein

The batch A1 of EV71 vaccine, the batch of EV71 vaccine stock solution, and aluminum adjuvant were taken; also the batch B1 of DTaP vaccine B, vaccine stock solutions of pertussis vaccine, diphtheria toxoid vaccine, and tetanus toxoid vaccine, as well as aluminum adjuvant were taken for detecting as per item 1.3.

The batch A1 of EV71 vaccine and the batch of EV71 vaccine stock solution were taken, as well as batch B1 of DTaP vaccine and pertussis vaccine, diphtheria toxoid vaccine, and tetanus toxoid vaccine stock solutions for detecting as per item 1.4.

### 2.6.2. Evaluation of Batch-to-Batch Consistency of EV71 Vaccine Particles

Four batches of final EV71 vaccine products (A1-A4) were tested according to item 1.3, and the CV of batch-to-batch D50 was calculated.

### 2.6.3. Evaluation of Batch-to-Batch Consistency of Vaccine Particles

The A1 batch of EV71 vaccine and the B1 batch of DTaP vaccine for testing as per item 1.3, and the CV of D50 within the batch was calculated.

### 2.6.4. Evaluation of Vaccine Particle Stability

#### 2.6.4.1. Long-Term Stability

The A1 batch of EV71 vaccine and the B1 batch of DTaP vaccine were taken that have been stored at 4 °C for 0, 3 months and 6 months for detecting as per item 1.3, and the CV of D50 were calculated.

#### 2.6.4.2. Accelerated Stability

The A1 batch of EV71 vaccine and the B1 batch of DTaP vaccine at 37 °C or -20 °C were placed for 1 day respectively and then detected the vaccine particle D50 as per item 1.3, which were compared with that under normal storage conditions (4 °C).

## 3. Results

### 3.1. Adsorption Effect of Aluminum Adjuvant on DPT Antigen Protein

The results showed that the particle size distribution of EV71 vaccine stock solution from Factory A was between 40 and 350 nm. The distribution range was extremely narrow ( $D_{90}/D_{10} \approx 2.2$ ), indicating that the particle size of the original solution was extremely uniform, which was an ideal state for vaccine particle size distribution. While the particle size distribution of the aluminum adjuvant was between 75 and 600 nm, which was larger than that of the vaccine stock solution. The particle size distribution of the EV71 vaccine finished product was between 50 and 14,000 nm, which was larger than that of the aluminum adjuvant. Moreover, this EV71 vaccine finished product exhibited a distinct bimodal distribution pattern. The main peak was at 0.1–0.2  $\mu\text{m}$ , accounting for approximately 65% of the volume, representing normal adjuvant particles. The secondary peak was at 0.3–3  $\mu\text{m}$ , accounting for approximately 14% of the volume, representing adjuvant aggregates/turbules. The results are shown in Figure 1.

The particle size of the diphtheria toxoid vaccine stock solution, pertussis vaccine stock solution and tetanus toxoid vaccine stock solution from Manufacturer B was distributed between 56 and 300 nm, while the particle size of the aluminum adjuvant was distributed between 56 and 630 nm, which was also slightly larger than that of the antigen protein particles. The particle size of the DTaP vaccine finished product was distributed between 2000 and 20000 nm, larger than that of the aluminum adjuvant. Moreover, the distribution range of the DTaP vaccine product is relatively wide. The main peak is at 3–8  $\mu\text{m}$ , accounting for 79.6% of the volume; the tail is above 8  $\mu\text{m}$ , accounting for 15.7% of

the volume. This result indicates that there is significant particle agglomeration in this product, with a high proportion of large particle aggregates (>15%). The results are shown in Figure 2.

The above results all indicated that the aluminum adjuvant had a good adsorption effect on the antigen protein. However, both of the two vaccines that were adsorbed with aluminum adjuvant exhibited obvious particle aggregation, with a relatively high proportion of aggregated particles, which may affect the homogeneity and injection safety of the vaccines.

According to the results of scanning electron microscopy, the particles of the two vaccines' stock solutions could not be observed by scanning electron microscopy, while the particles of the finished products with added aluminum adjuvant could be clearly seen. The results were shown in Figure 3. Therefore, the scanning electron microscopy results also indicated that the aluminum adjuvant had a good adsorption effect on the antigen protein.

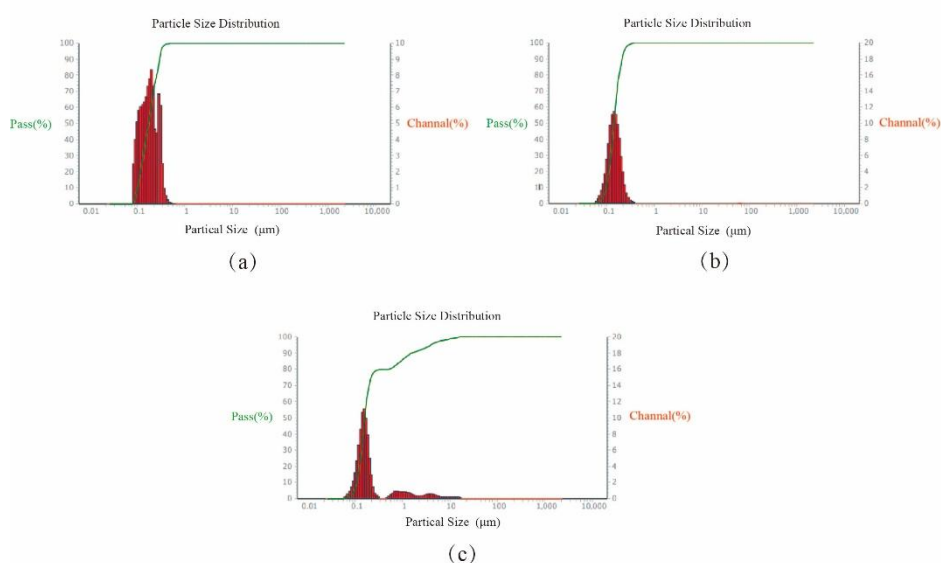


**Figure 1.** Particle size distribution of EV71 vaccine. (a), (b), (c) represents respectively the particle size distribution of EV71 vaccine adjuvant, EV71 vaccine stock solution, and EV71 vaccine finished product.

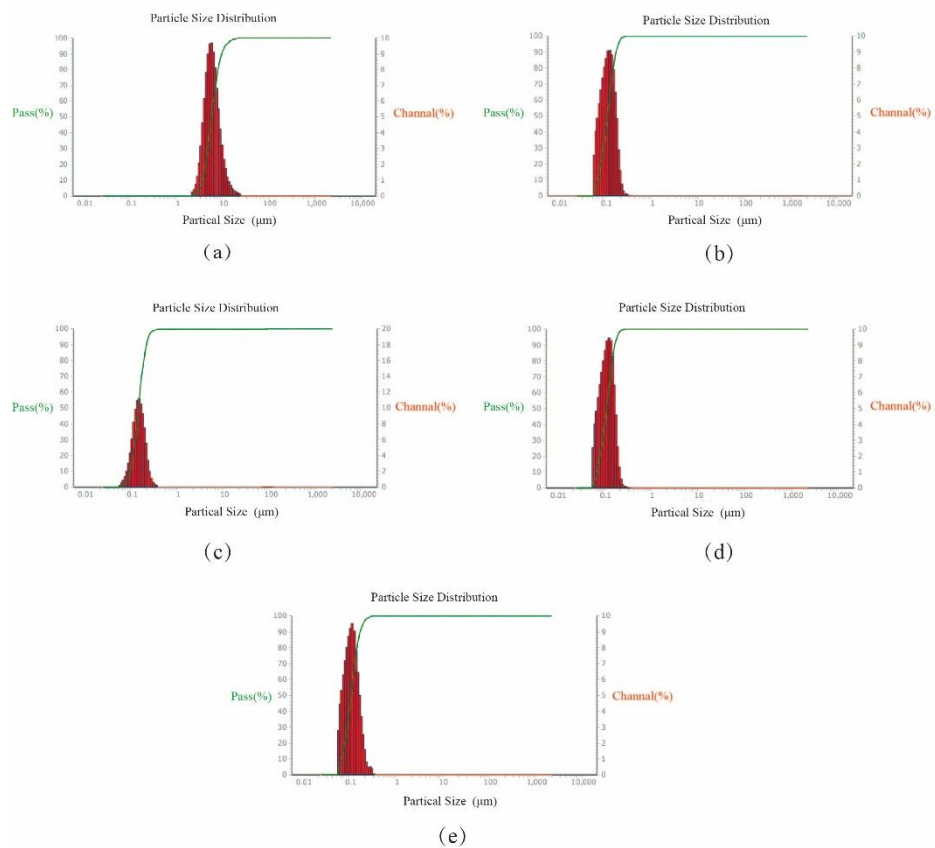


**Figure 2.** Particle size distribution of DTaP vaccine. (a), (b), (c), (d) and (e) represents respectively the particle size distribution diagram of the DTaP vaccine adjuvant, DTaP vaccine finished product, the diphtheria toxoid vaccine stock solution, pertussis vaccine stock solution and the tetanus toxoid vaccine stock solution.

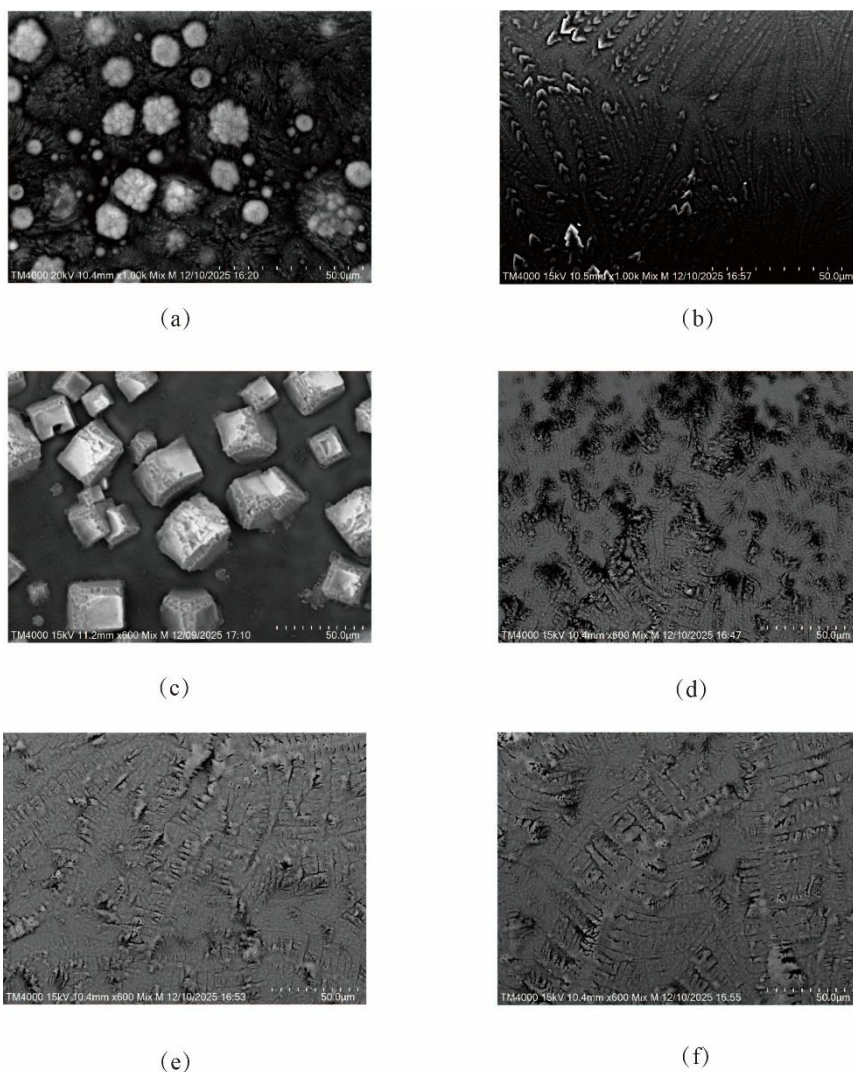


**Figure 3.** Scanning electron microscope image of the vaccine. (a), (b), (c), (d), (e) and (f) represents respectively the electron microscope scan image of the finished product of the EV71 vaccine, EV71 vaccine stock solution, DTaP vaccine finished product, the pertussis vaccine stock solution, the diphtheria vaccine stock solution and the tetanus toxoid vaccine stock solution.

### 3.2. Consistency of Finished Vaccine Particles

#### 3.2.1. Batch-to-Batch Consistency

The results showed that the D50 values of EV71 vaccine batches A1 to A4 were 100, 132, 103, and 103 nm respectively. The peak shapes of the particle size distribution graphs varied significantly, and the CV of the D50 values of the 4 batches of vaccine particles was 13.8%, which was greater than 10%. As shown in Figure 4, this indicated that the particle distributions of the 4 batches of vaccines were not uniform.

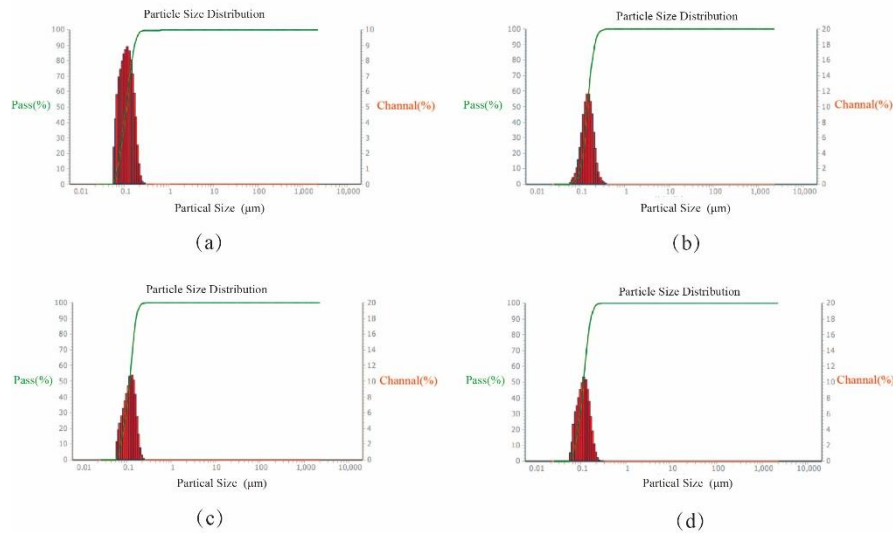


**Figure 4.** Particle size distribution of EV71 vaccine. (a), (b), (c) and (d) represents the particle size distribution of EV71 vaccine batches A1-A4, respectively.

### 3.2.2. Batch-to-Batch Consistency

The results showed that the D50 values of the three bottles of EV71 vaccine batch A1 and batch D50 were 109, 101, and 107 nm respectively, with the CV of 3.9% for D50. The D50 values of the three bottles of DTaP vaccine batch B1 were 3.72, 3.62, and 3.19  $\mu\text{m}$  respectively, with the CV of 8.0%. As shown in Figure 5, This indicated that the batch-to-batch consistency of the two vaccines was good, and the filling operation did not cause significant changes in the particle size and distribution of the vaccines.

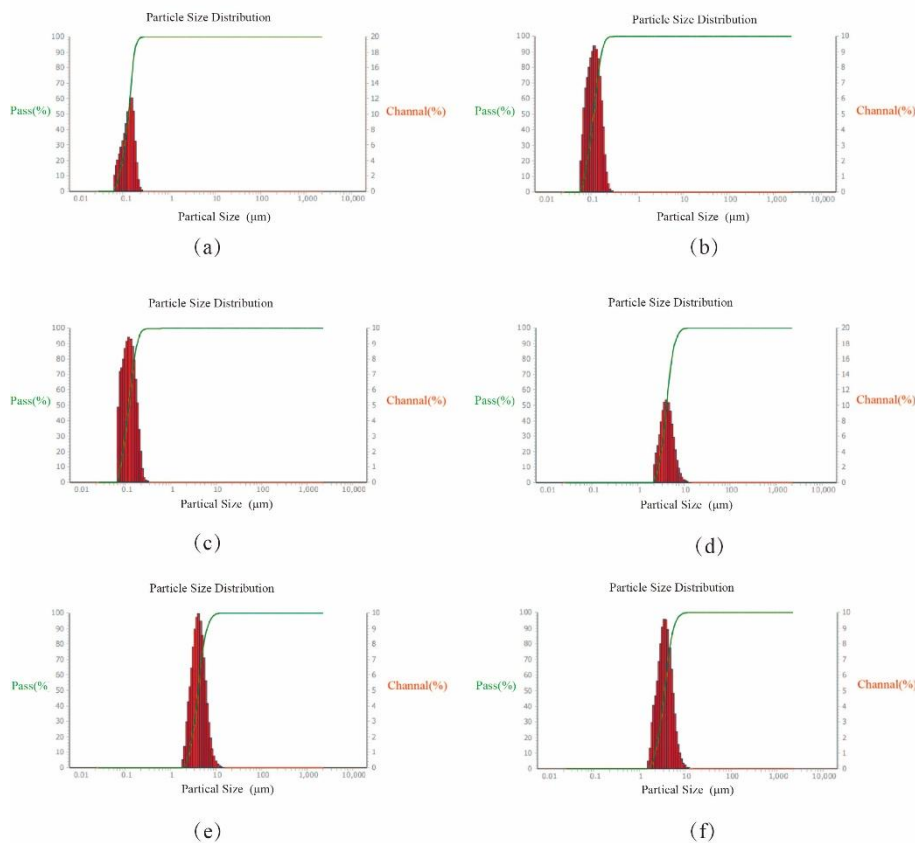


**Figure 5.** Particle size distribution of different vaccines. (a), (b) and (c) represents the particle size distribution graphs of the EV71 vaccine finished product batch A1 measured three times respectively. (d), (e) and (f) represents the particle size distribution graphs of the DTaP1 vaccine finished product batch B1 measured three times respectively.

### 3.3. Stability of Vaccine Particles

#### 3.3.1. Long-Term Stability

The results showed that for the EV71 vaccine batch A1, the D50 of the particles after storage for 0, 30, and 60 days were 100, 114 and 134 nm respectively, with the CV of 14.7% for D50. However, on the 0th day, the aggregates larger than 0.2  $\mu\text{m}$  accounted for only 0.03% and the product was almost free of agglomeration; on the 30th day, the aggregates larger than 0.2  $\mu\text{m}$  increased to 0.85%, increasing by approximately 28 times, and began to form aggregates; on the 60th day, the aggregates larger than 0.2  $\mu\text{m}$  reached 1.50%, and large particles larger than 10  $\mu\text{m}$  (0.38%) appeared, suggesting a serious risk of agglomeration. The finished EV71 vaccine showed a significant tendency of particle aggregation during storage.

For the DTaP vaccine batch B1, the D50 of the particles after storage for 0, 30, and 60 days were 4.82, 5.39 and 4.77  $\mu\text{m}$  respectively, with the CV of 6.9%. However, on the 0th day, the main peaks were concentrated in the range of 4-10  $\mu\text{m}$ , and those larger than 20  $\mu\text{m}$  accounted for only 0.4%. The product quality was good, and the peaks were symmetrical. On the 30th day, the main peaks shifted to 5.5-7  $\mu\text{m}$ , and the proportion of 6-10  $\mu\text{m}$  increased to 38.4%, starting to aggregate. On the 60th day, a severe tail was observed, with particles larger than 50  $\mu\text{m}$  accounting for 2.8%, and those in the range of 20-50  $\mu\text{m}$  increased to 2.6%.

The results are shown in Figure 6. The long-term stability results of the two vaccines indicated that D50 did not change significantly during storage, suggesting that the long-term storage stability of the vaccines was good. However, the particles will gradually aggregate over time, thereby affecting the stability and safety of the vaccines.

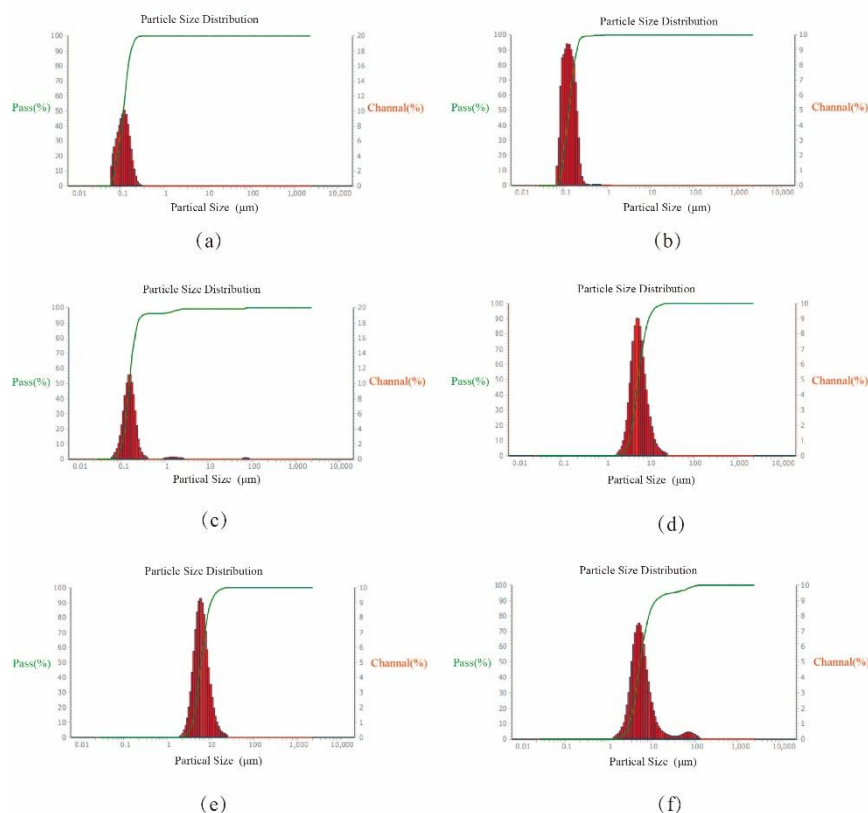


**Figure 6.** Particle size distribution of different vaccines at different storage times. (a), (b) and (c) represents the particle size distribution graphs of the EV71 vaccine product batch A1 at 0, 30, and 60 days of storage, respectively. (d), (e) and (f) represents the particle size distribution graphs of the DTaP vaccine product batch B1 at 0, 30, and 60 days of storage, respectively.

### 3.3.2. Accelerated Stability

The D50 values of the vaccine particles of batch A1 of EV71 vaccine at 37 °C were 3.44 and 3.24 μm respectively, with the CV of 4.2%. Both of these values were higher than the D50 values (101 and 98 nm respectively, with the CV of 2.1%) under the 4 °C storage condition. Moreover, the particle size distribution was uneven. The D50 values of the vaccine particles of batch A1 of EV71 vaccine at -20 °C were 33.27 and 41.81 μm respectively. Compared with the storage conditions at 4 °C and 37 °C, the particle sizes of the vaccine particles were significantly larger, with the CV of 16.1%, and the CV also increased significantly, as shown in Figure 7.

The D50 values of the vaccine particles of batch B1 of DTaP vaccine at 37 °C were 9.11 and 8.60 μm respectively, with a CV of 4.1%. Both of these values were higher than those under 4 °C storage conditions (D50 was 3.52 and 3.18 μm respectively, with the CV of 7.2%), and the particle size distribution was uneven. The D50 values of the vaccine particles of batch B1 of DTaP vaccine at -20 °C were 41.04 and 49.95 μm respectively. Compared with the storage conditions at 4 °C and 37 °C, the particle sizes of the vaccine particles were significantly larger, with the CV of 13.8%, and the CV also increased significantly, as shown in Figure 8.

The above results indicated that the placement at 37 °C had a relatively minor impact on the stability of the vaccine particle size, but it would result in an uneven distribution of particle sizes. Under the freezing condition of -20 °C, the particle size of the vaccine was significantly affected.

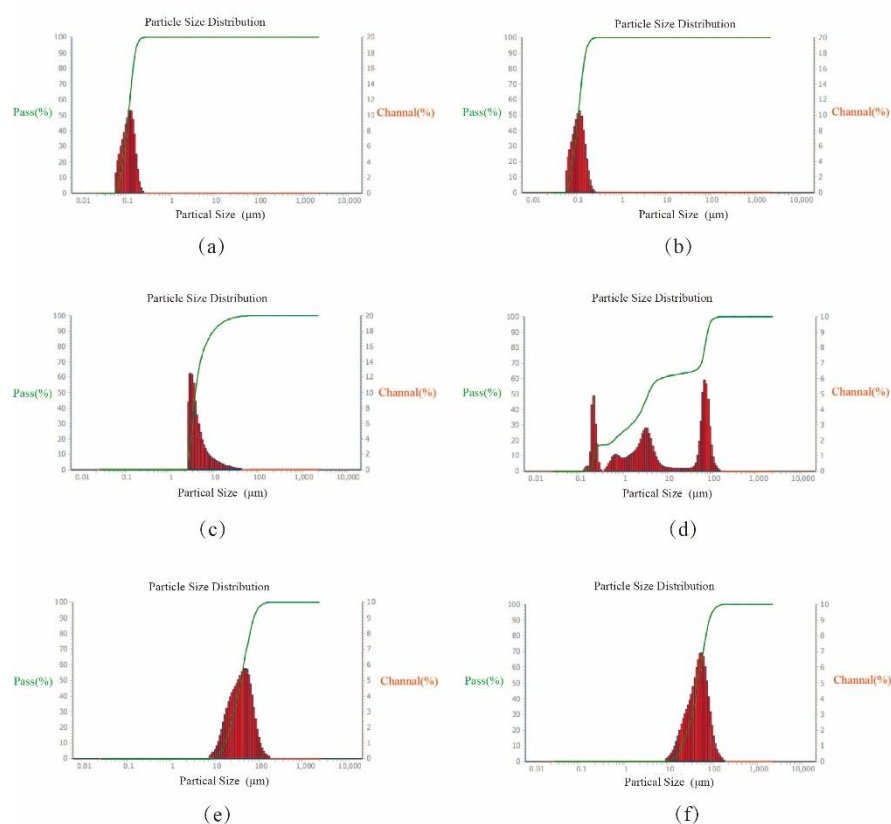


**Figure 7.** Particle size distribution diagram of EV71 vaccine at different temperatures. (a) and (b) represents the particle size distribution diagrams of the EV71 vaccine product batch A1 after being stored at 4 °C. (c) and (d) represents the particle size distribution diagrams of the same batch after being stored at 37 °C for one day. (e)

and (f) represents the particle size distribution diagrams of the same batch after being stored at -20 °C for one day.

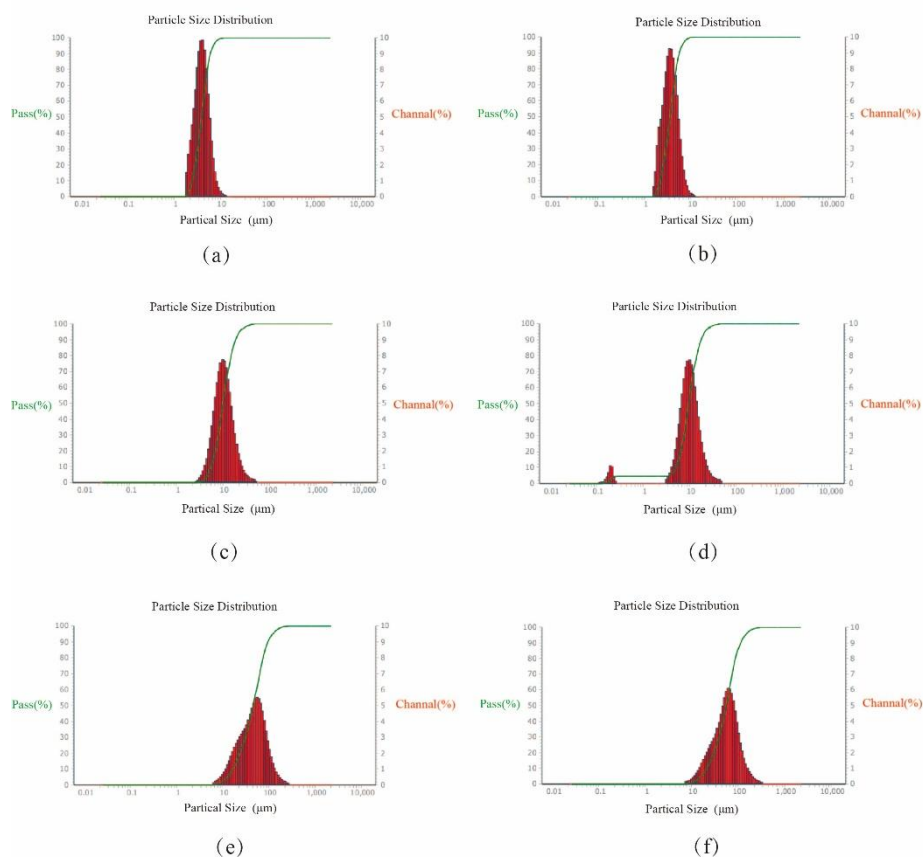


**Figure 8.** Particle size distribution diagram of DTaP vaccine at different temperatures. (a) and (b) represents the particle size distribution diagrams of the DTaP vaccine product batch B1 after being stored at 4 °C. (c) and (d) represents the particle size distribution diagrams of the same batch after being stored at 37 °C for one day. (e) and (f) represents the particle size distribution diagrams of the same batch after being stored at -20 °C for one day.

#### 4. Discussion

Dynamic laser scattering method can be used for the characterization of biological macromolecules such as proteins, antibodies, and viruses. Its advantages lie in its speed, non-destructiveness, and the ability to measure extremely small particles. The data from the studies on the DTaP vaccine containing aluminum hydroxide oxide (AlO(OH)) adjuvant (Table 2) [26] and the quadrivalent/quivalent vaccine containing aluminum phosphate (AlPO<sub>4</sub>) adjuvant (Table 3) [27] showed that DLS could detect the nanoscale size changes of the antigens, while LD is more suitable for characterizing the micrometer-sized aggregates after adjuvantization, and SEM provides direct evidence of surface adsorption morphology.

**Table 2.** Comparison of Different Methods for Detecting Aluminum Hydroxide Oxide (AlOOH) Adjuvant in Diphtheria-Pertussis-Tetanus Vaccine.

| Method | Measuring object                                 | Particle size results       | Conclusion   |
|--------|--|-----------------------------|--|
| DLS    | Genetic detoxification of pertussis toxin (gdPT) | 9.3 nm and 320 nm (bimodal) | Nanometer-sized particles capable of detecting free antigens |

| Method | Measuring object                           | Particle size results | Conclusion   |
|--------|--|-----------------------|--|
| DLS    | PT   | 440 nm                | Antigen aggregation state                                    |
| LD     | After being adsorbed by the AIOOH adjuvant | 3.5–22 $\mu\text{m}$  | The adjuvant determines the final particle size distribution |

**Table 3.** Comparison of Different Methods for Detecting Tetra-/Penta-valent Vaccines Containing Phosphate Aluminum ( $\text{AlPO}_4$ ) Adjuvant.

| Method | Measuring results                    | Conclusion   |
|--------|--------------------------------------|--|
| DLS    | Antigen hydrodynamic diameter        | 7–182 nm (wide distribution)                         |
| LD     | After adjuvantization, particle size | 10–12 $\mu\text{m}$ (narrow distribution)            |
| SEM    | morphologic observation              | Submicron particles form a continuous porous surface |

This study utilized the laser particle size analyzer and a scanning electron microscope to analyze the particle size and distribution of the inactivated enterovirus 71 vaccine stock solution, DTP vaccine stock solution, the aluminum adjuvant, and the final vaccine product. The adsorption effect of the adjuvant on the antigen protein in the final product was evaluated. The results indicated that the aluminum adjuvant had a good adsorption effect on the antigen protein. However, compared with the vaccine stock solution, although the aggregation degree of the two vaccine finished product particles was different, after adding sodium hydroxide adjuvant to the vaccine stock solution, there may be a phenomenon of particle aggregation, and the aggregated particles account for a relatively high proportion, which may affect the homogeneity and injection safety of the vaccine.

This study compared the D50 values of EV71 vaccine particles to evaluate the batch-to-batch consistency. It was found that the particle distribution of EV71 vaccines from the same manufacturer was uneven. Therefore, this finding can be used to guide process improvement and enhance the consistency between different batches. Additionally, by comparing the D50 values of the same batch of two vaccines, it was discovered that the batch-to-batch consistency of EV71 vaccine and DTaP vaccine was good, indicating that the filling and packaging process has little impact on the particle distribution of different vaccines.

In the stability experiment, the two vaccine products exhibited a distinct tendency of particle aggregation during storage over time, which was consistent with the stability characteristics of vaccines as reported in the literature[28,29]. Therefore, this study suggests that the particle size distribution should be monitored regularly, especially the proportion of aggregates larger than 20  $\mu\text{m}$ . In addition, the particle size of the vaccine should be measured using a laser particle size analyzer based on the existing standards. Besides detecting the D50 coefficient, it is also necessary to establish release standards for the D10 and D90 coefficients to ensure the homogeneity and injection safety of the vaccine. At the same time, for vaccines that need to be stored for a long time, due to the presence of ultra-large particles larger than 50  $\mu\text{m}$ , safety and efficacy evaluations should be conducted. If necessary, consideration should be given to disposal.

On the other hand, the main reason for the impact of low temperature on the stability of the vaccines is that low temperature damages the structure of the adjuvant and the antigen. Both vaccines were kept at  $-20\text{ }^\circ\text{C}$ , and the particles significantly increased in size, which had a significant impact on the stability of the vaccine particles. Therefore, if the vaccines are exposed to an environment of  $-20\text{ }^\circ\text{C}$  or below, it will cause changes in the particle size and distribution of the vaccines. Therefore, especially for vaccines with adjuvants, strictly controlling the temperature during transportation and storage is very important for the stability of the vaccine particles[30].

When stored at  $37\text{ }^\circ\text{C}$ , the particle size will slightly increase and the distribution will become less uniform. At the same time, study has shown that  $37\text{ }^\circ\text{C}$  will accelerate the aging of the adjuvant[28].

Therefore, the vaccine should not be exposed to normal temperature for a long time[31]. For example, when the refrigerator loses power and then returns to room temperature, the vaccine should be promptly transferred to the specified temperature for storage.

Based on the particle size results obtained from the laser particle size analyzer for the two vaccines, in the future, the production process of the vaccines can be improved by adding cryoprotectants (such as propylene glycol[32]), which can effectively prevent aggregation caused by freeze-thaw cycles. However, further consideration is needed to determine whether the addition of stabilizers will have any impact on the safety, efficacy and particle size of the vaccine. At the same time, by optimizing the dispersion process of the adjuvant, the initial agglomeration can be reduced. Moreover, since the particle size of nano-sized aluminum hydroxide is only 110-140 nm, which has a larger specific surface area and stronger adsorption capacity than the conventional aluminum hydroxide adjuvant[33], this adjuvant can be considered to replace the existing one in the future.

## 5. Conclusion

This study used the laser particle size analyzer to evaluate the size of vaccine particles. Based on the detection method for insoluble particles in the Chinese Pharmacopoeia (2025 edition), a new method for evaluating the particle size distribution of vaccines has been established. Due to its wide measurement range and the ability to measure extremely small particles, it also has guiding significance for evaluating the consistency of the production process and the stability of the product regarding the size and distribution of vaccine particles.

**Author Contributions:** Conceptualization, Li Xinwei. and Su Wen.; methodology, Su Wen.; software, Fang Wei.; validation, Li Xinwei., Fang Wei. and Su Wen.; formal analysis, Wang Enna.; investigation, Zeng Haiyuan.; resources, Song Jie.; data curation, Li Xinwei.; writing—original draft preparation, Li Xinwei.; writing—review and editing, Su Wen.; visualization, Fang Wei.; supervision, Wu Fan.; project administration, Su Wen.; funding acquisition, Su Wen.

**Funding:** This research was funded by the project #202002AA100008 and #2024-KYYJ-005 approved by the Yunnan Provincial Government of China, respectively.

**Acknowledgement:** Authors would like to thank China Institute of Medical Biology, Chinese Academy of Medical Sciences, for their initial work towards particle size distribution of adjuvants and their support. Song Jie, He Xinwen and Fan Bo are thanked for their support during experimental set up and for scientific discussions.

**Conflicts of Interest:** The funders had no role in the design of the study; in the collection, analyses, or interpretation of data; in the writing of the manuscript; or in the decision to publish the results.

## Reference

1. Tambyah, P. A. et al. An inactivated enterovirus 71 vaccine is safe and immunogenic in healthy adults: A phase I, double blind, randomized, placebo-controlled, study of two dosages. *Vaccine* **37**, 4344–4353 (2019). <https://doi.org/10.1016/j.vaccine.2019.06.023>
2. Liang, Z. & Wang, J. EV71 vaccine, an invaluable gift for children. *Clinical & Translational Immunology* **3** (2014). <https://doi.org/10.1038/cti.2014.24>
3. Zheng, D. et al. Effect of EV71 Vaccination on Transmission Dynamics of Hand, Foot, and Mouth Disease and Its Epidemic Prevention Threshold. *Vaccines* **12** (2024). <https://doi.org/10.3390/vaccines12101166>
4. Prygiel, M., Mosiej, E., Górska, P. & Zasada, A. A. Diphtheria–Tetanus–Pertussis Vaccine: Past, Current & Future. *Future Microbiology* **17**, 185–197 (2021). <https://doi.org/10.2217/fmb-2021-0167>

5. Godfroid, F., Denoël, P., de Grave, D., Schuerman, L. & Poolman, J. Diphtheria-tetanus-pertussis (DTP) combination vaccines and evaluation of pertussis immune responses. *International Journal of Medical Microbiology* **294**, 269–276 (2004). <https://doi.org/10.1016/j.ijmm.2004.07.007>
6. Mohanty, L. et al. A randomized, open-label clinical trial to evaluate immunogenicity and safety of an indigenously developed DTwP-Hib tetravalent combination vaccine (Easyfour®-TT) with Quadrovax® in Indian infants. *Human Vaccines & Immunotherapeutics* **13**, 2025–2031 (2017). <https://doi.org/10.1080/21645515.2017.1342020>
7. Loiacono, M. M., Pool, V. & van Aalst, R. DTaP combination vaccine use and adherence: A retrospective cohort study. *Vaccine* **39**, 1064–1071 (2021). <https://doi.org/10.1016/j.vaccine.2021.01.009>
8. Szejser-Zawislak, E. et al. Evaluation of Whole-Cell and Acellular Pertussis Vaccines in the Context of Long-Term Herd Immunity. *Vaccines* **11** (2022). <https://doi.org/10.3390/vaccines11010001>
9. Monteiro, S. A. M. G., Takano, O. A. & Waldman, E. A. Surveillance for adverse events after DTwP/Hib vaccination in Brazil: Sensitivity and factors associated with reporting. *Vaccine* **28**, 3127–3133 (2010). <https://doi.org/10.1016/j.vaccine.2010.02.059>
10. Chen, R. T. et al. Enhancing vaccine safety capacity globally: A lifecycle perspective. *Vaccine* **33**, D46–D54 (2015). <https://doi.org/10.1016/j.vaccine.2015.06.073>
11. Ferrari, F. et al. Bayesian hierarchical model predicts biopharmaceutical stability indicators and shelf life with application to multivalent human papillomavirus vaccine. *Scientific Reports* **15** (2025). <https://doi.org/10.1038/s41598-025-99458-y>
12. Shah, R. R., O'Hagan, D. T. & Brito, M. M. A. L. A. The impact of size on particulate vaccine adjuvants. *Nanomedicine* **9**, 2671–2681 (2014).
13. Misra, R., Fung, G., Sharma, S., Hu, J. & Kirkitadze, M. Assessment of Tunable Resistive Pulse Sensing (TRPS) Technology for Particle Size Distribution in Vaccine Formulations – A Comparative Study with Dynamic Light Scattering. *Pharmaceutical Research* **41**, 1021–1029 (2024). <https://doi.org/10.1007/s11095-024-03698-y>
14. Mei, C. et al. Aluminum Phosphate Vaccine Adjuvant: Analysis of Composition and Size Using Off-Line and In-Line Tools. *Computational and Structural Biotechnology Journal* **17**, 1184–1194 (2019). <https://doi.org/10.1016/j.csbj.2019.08.003>
15. Havlik, M. et al. Comprehensive Size-Determination of Whole Virus Vaccine Particles Using Gas-Phase Electrophoretic Mobility Macromolecular Analyzer, Atomic Force Microscopy, and Transmission Electron Microscopy. *Analytical Chemistry* **87**, 8657–8664 (2015). <https://doi.org/10.1021/acs.analchem.5b01198>
16. Lancaster, C., Rustandi, R. R., Pannizzo, P. & Ha, S. in *Clostridium difficile Methods in Molecular Biology* Ch. Chapter 21, 279–287 (2016).
17. Commission, C. P. *Pharmacopoeia of the People's Republic of China*. (China Medical Science and Technology Press, 2025).
18. Ripple, D. C., Montgomery, C. B. & Hu, Z. An Interlaboratory Comparison of Sizing and Counting of Subvisible Particles Mimicking Protein Aggregates. *Journal of Pharmaceutical Sciences* **104**, 666–677 (2015). <https://doi.org/10.1002/jps.24287>
19. Levin, I., Zigman, S., Komlos, A. & Kettenring, J. Development of Flow Imaging Analysis for Subvisible Particle Characterization in Glatiramer Acetate. *Journal of Pharmaceutical Sciences* **104**, 3977–3983 (2015). <https://doi.org/10.1002/jps.24550>
20. Sharma, D. K., Oma, P., Pollo, M. J. & Sukumar, M. Quantification and Characterization of Subvisible Proteinaceous Particles in Opalescent mAb Formulations Using Micro-Flow Imaging. *Journal of Pharmaceutical Sciences* **99**, 2628–2642 (2010). <https://doi.org/10.1002/jps.22046>
21. Hayek, H. et al. Vaccine Adjuvants in the Immunocompromised Host: Science, Safety, and Efficacy. *Transplant Infectious Disease* **27**, e70053 (2025). <https://doi.org/10.1111/tid.70053>
22. Clapp, T., Siebert, P., Chen, D. & Jones Braun, L. Vaccines with Aluminum-containing Adjuvants: Optimizing Vaccine Efficacy and Thermal Stability. *Journal of Pharmaceutical Sciences* **100**, 388–401 (2011). <https://doi.org/10.1002/jps.22284>

23. Filippov, S. K. et al. Dynamic light scattering and transmission electron microscopy in drug delivery: a roadmap for correct characterization of nanoparticles and interpretation of results. *Materials Horizons* **10**, 5354–5370 (2023). <https://doi.org/10.1039/d3mh00717k>
24. George, A., Alva, E., Brancaleon, L. & Marucho, M. Dynamic and electrophoretic light scattering measurements on microtubules at low concentrations. *PLOS ONE* **19**, 1–18 (2024). <https://doi.org/10.17504/protocols.io.dm6gpzrqjlp/v1>
25. Stetefeld, J., McKenna, S. A. & Patel, T. R. Dynamic light scattering: a practical guide and applications in biomedical sciences. *Biophysical Reviews* **8**, 409–427 (2016). <https://doi.org/10.1007/s12551-016-0218-6>
26. Duprez, J. et al. Structure and compositional analysis of aluminum oxyhydroxide adsorbed pertussis vaccine. *Computational and Structural Biotechnology Journal* **19**, 439–447 (2021). <https://doi.org/10.1016/j.csbj.2020.12.023>
27. Kalbfleisch, K. et al. Identity, Structure and Compositional Analysis of Aluminum Phosphate Adsorbed Pediatric Quadrivalent and Pentavalent Vaccines. *Computational and Structural Biotechnology Journal* **17**, 14–20 (2019). <https://doi.org/10.1016/j.csbj.2018.11.006>
28. Xifei Yang, F. Z. Effects of storage temperature on the quality stability of nanoparticle aluminum hydroxide adjuvant. *Journal of Chinese Pharmaceutical Sciences* **34** (2025). <https://doi.org/10.5246/jcps.2025.10.067>
29. Kartoğlu, Ü. *Temperature Sensitivity of the Diphtheria Containing Vaccines*. (2012).
30. Fortpied, J. et al. Stability of an aluminum salt-adjuvanted protein D-conjugated pneumococcal vaccine after exposure to subzero temperatures. *Human Vaccines & Immunotherapeutics* **14**, 1243–1250 (2018). <https://doi.org/10.1080/21645515.2017.1421878>
31. Ahl, P. L. et al. Accelerating Vaccine Formulation Development Using Design of Experiment Stability Studies. *Journal of Pharmaceutical Sciences* **105**, 3046–3056 (2016). <https://doi.org/10.1016/j.xphs.2016.06.014>
32. Xue, H., Yang, B., Kristensen, D. D. & Chen, D. A freeze-stable formulation for DTwP and DTaP vaccines. *Human Vaccines & Immunotherapeutics* **10**, 3607–3610 (2015). <https://doi.org/10.4161/21645515.2014.980195>
33. HogenEsch, H., O'Hagan, D. T. & Fox, C. B. Optimizing the utilization of aluminum adjuvants in vaccines: you might just get what you want. *npj Vaccines* **3** (2018). <https://doi.org/10.1038/s41541-018-0089-x>

**Disclaimer/Publisher's Note:** The statements, opinions and data contained in all publications are solely those of the individual author(s) and contributor(s) and not of MDPI and/or the editor(s). MDPI and/or the editor(s) disclaim responsibility for any injury to people or property resulting from any ideas, methods, instructions or products referred to in the content.